Caving 2022 - Y Potvin (ed.)

doi:10.36487/ACG_repo/2205_86

Experimental investigation of hydraulic fracturing in granite under hydrostatic stress conditions

Z Ali *The University of Adelaide, Australia*

M Karakus *The University of Adelaide, Australia*

Abstract

Cave propagation and rock mass fragmentation are the major challenges in block cave mining. In deep underground mines where the rock mass is stronger and stresses are higher, an artificial weakening is required. Hydraulic fracturing (HF) has evolved as one of the most preferred methods of preconditioning in block cave mining as it provides better control of fracture geometry and orientation and helps in the dissipation of the stored excess strain energy. The breakdown pressure, fracture propagation and orientation are some of the important parameters which govern the success of HF operations. In order to understand these parameters and to collect reliable data for numerical investigations, laboratory-scale HF experiments were performed on cylindrical samples of Adelaide black granite under various hydrostatic stress conditions. A borehole of 8 mm in diameter and 63.5 mm in length was pressurised using dyed water until the specimen failed under four different confining pressures. The failure process was monitored using an acoustic emission monitoring system with several piezoelectric sensors in order to characterise the fracturing process during the experiments. A positive linear relationship was observed between the breakdown pressure and the hydrostatic stresses which is in line with the theoretical results. However, it was observed that the rock tensile strengths found using Brazilian disc tests are slightly lower than the breakdown strengths.

Keywords: *block caving, preconditioning, de-stressing, hydraulic fracturing, acoustic emission*

1 Introduction

Block caving is applied to ore bodies which can fragment and cave under the influence of gravity and in situ stresses. With mines getting deeper and rock getting stronger, the challenges of natural caving are getting more pronounced and geotechnical risks such as caving hang-up, uncontrolled caving and rock bursts have more potential to happen. The key to success in block cave mining is the cave initiation pattern and its propagation (Brady & Brown 1999). For better management of the caving process and to minimise the inherent geotechnical risks of cave mining, a technique known as preconditioning can be used. The preconditioning (also known as de-stressing) of the rock mass can be undertaken by hydraulic fracturing, blasting, thermal treatment or using a combination. Though all the techniques of de-stressing can be effective in the right application, there are circumstantial evidence that hydraulic fracturing is beneficial in some rock masses. Hydraulic fracturing is a prominent method of fracturing in the shale gas industry, and it was first successfully applied in 1949 (Clark 1949). The method is also used for measuring in situ stresses, stimulating groundwater wells, enhancing hydrocarbon and geothermal energy extraction, and injection rates for hazardous solid waste disposal (Chacon et al. 2004; Mills 2004). In the mining industry, hydraulic fracturing has been used for preconditioning hard rock masses to facilitate caving, reduce seismic risks and to improve fragmentation in block cave mines (Catalan et al. 2017a; Jeffrey et al. 2017; Mills 2004). However, its use in mining industry is not limited to cave mining only, as the method is extensively used in coal mining for controlling roof collapse, methane extraction and increasing rock permeability (Zhai et al. 2012).

The basic concept of hydraulic fracturing is to pressurise a borehole until it surpasses the tensile strength of the rock and the rock breaks. A high-pressure liquid is used to pressurise the borehole column until cracks emerge in the rock. The process of injecting pressurised fluid is continued in the cracks, which extend the cracks further into the rock formation until the desired limits have been reached (Brzovic et al. 2015). In block

cave mining, preconditioning is done by drilling multiple boreholes into the orebody to create several transverse fractures from each drilled borehole. The new fractures are created to improve the natural caving and fragmentation of the orebody, which is key to the success of this mining method (He et al. 2016a; Juncal et al. 2014). The mechanism of hydraulic fracturing is complex and depends on a number of parameters that can influence the performance of hydraulic fractures, as studied and identified by (Bunger et al. 2011).

This research investigates the breakdown pressure in Adelaide black granite under different hydrostatic stress conditions and acoustic emission (AE) characterisation of the fracturing process. The paper is divided into four sections. Section two briefly describes hydraulic fracturing and introduces the governing equations used in the study. In section three, sample is introduced, and the experimental procedure is described. Section four presents the results and detailed discussion, which is followed by the conclusion.

2 Hydraulic fracturing

Hydraulic fracturing is undertaken by injecting high-pressure fluid into a rock mass until the rock fails. A borehole is drilled, and a desired portion of the borehole is isolated generally using a set of inflatable packers as shown in Figure 1. According to Katsaga et al. (2015) a fracture is created when the injected fluid pressure surpasses the tensile or shear strength of the surrounding rock. These tensile stresses are generated by the combination of in situ stresses and porewater pressure around the borehole and fluid pressure inside the borehole. Besides the major faults and joints, the rock formations have micro-cracks and one basic assumption about hydraulic fracturing is that the tensile cracks generated are basically the generation and growth of the existing micro-cracks. This assumption was adopted during the experiments and the generation and growth of the micro-cracks were monitored through AE and correlated with the results.

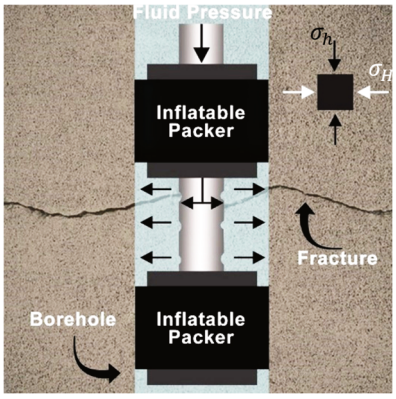

(a)

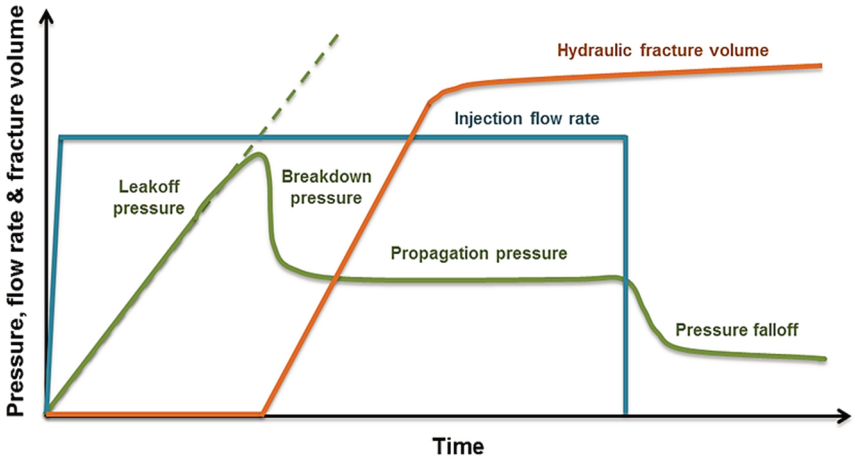

(b)

Figure 1 (a) Schematic of hydraulic fracturing; (b) Conceptual breakdown pressure curve

To locate the effective hydraulic fracturing zones and to create optimal fracture network within the rock mass it is important to predict the breakdown pressure or the maximum internal pressure the rock mass can withstand. The breakdown pressure is an important parameter that governs the fracturing process in rocks and is usually plotted against the time as shown in Figure 1. However, there are several other factors which can influence the process like the injection rate, fluid properties, rock mass properties and most importantly the in situ stress conditions. The rock mass in the earth crust is subjected to three principal stresses; a compressive principal stress in the vertical direction due to overlaying strata, σ_v, and two horizontal principal stresses known as major horizontal principal stress, σ_H and minor horizontal principal stress, σ_h. The most frequently adopted theory to estimate the breakdown pressure for a vertical borehole utilises this spatial stress tensor presented as under:

Breakdown pressure = (Tensile Strength) + (Magnitude of Stresses) – 2 × (Difference of Stresses) – (Porewater Pressure)

$$P_b = (\sigma_h + \sigma_H) + 2(\sigma_h - \sigma_H) - P_p + T \quad (1)$$

$$P_b = 3\sigma_h - \sigma_H - P_p + T \quad (2)$$

Where P_b is the breakdown pressure, P_p is the pore pressure and T is the tensile strength of the rock. Equation 1 shows that for a vertical borehole, the horizontal stresses are the governing factors in hydraulic fracturing and can influence the breakdown pressure more than the tensile strength of the rock. The equation also tells us that the difference in stresses is twice as important as the magnitude of the stresses and that breakdown pressure is not affected by the vertical stresses. Under the hydrostatic stress states, σ_h is theoretically equal to σ_H and for dry samples, the porewater pressure is assumed to be negligible. Therefore, Equation 2 under the hydrostatic stress conditions becomes:

Initiation Pressure = 3 (Confining Pressure)-Confining Pressure + Tensile Strength

$$P_b = 2\sigma_H + T \quad (3)$$

The model can predict the breakdown pressure, however when the tensile strength is back calculated using this expression, the values are found to be greater than the measured strengths using Brazilian disc tests. Also, the above relationship implies that the breakdown pressure would yield a gradient of two when plotted against the hydrostatic pressure. However, studies show that the breakdown pressure yields a gradient of 1 when plotted against confining stresses (Stoeckhert et al. 2014; Mehrgini et al. 2016). An approach that yields a gradient of 1 is from the Haimson & Fairhurst (1967) approach of continuum mechanics. According to Haimson the breakdown pressure for the non-porous and impermeable rock can be given by:

$$P_b = \frac{3\sigma_h - \sigma_H + \mathrm{T}}{2} \quad (4)$$

A more precise model was presented by Adam et al. (2017) which is based on fracture mechanics and the theory of critical distances as under:

$$P_b = \sigma_n + T + \frac{K_{IC}}{2}\sqrt{\frac{4}{\pi(R + a_{ic})}} \quad (5)$$

Where σ_n is the minor principal stress, K_{IC} is the mode I fracture toughness of the rock, R is the radius of the bore hole and a_{ic} is the critical length of the initial fracture from the borehole wall defined as under:

$$a_{ic} = \frac{1}{2\pi}\left(\frac{K_{IC}}{T}\right)^2 \quad (6)$$

The mode I fracture toughness for a semi-circular bend (SCB) specimen is given by:

$$\mathrm{K}_{IC} = \sigma \mathrm{Y}' \sqrt{\pi a} \quad (7)$$

where a is the initial crack length, σ is the applied stress and Y' is geometrical parameter given by:

$$\mathrm{Y}' = 4.782 - 1.219\left(\frac{a}{r}\right) + 0.063^{7.045\left(\frac{a}{r}\right)} \quad (8)$$

In this study, the breakdown values are predicted using Equations 3, 4 and 5 which are then compared to the experimental results.

3 Experimental investigation

3.1 Sample preparation

The specimens were prepared from the Adelaide black granite because of its high strength and low permeability as the hydraulic fracture experiments were likely to fail with any of the high permeable rock samples because of the water infiltration into pores. The Adelaide black granite is a fine-grained black rock with a very low water absorption by weight of approximately 0.03%. The rock is very dense with a bulk density of 2.97 tonnes/m^3, an average compressive strength of 184.9 MPa and average tensile strength of 11.8 MPa as shown in Table 1. The petrographic analysis of the samples shows that the rock contains 67% plagioclase, 15% clinopyroxene (augite), 10% orthopyroxene, 5% K feldspar, 1% biotite, 1% ilmenite, and 1% other minerals (Ali et al. 2022). The samples were cored from the rock block using a 63.5 mm inner diameter drill bit, which were further sawn to the length of 127 mm to achieve a diameter to length ratio of 2. A centre hole of 8 mm diameter was drilled in the samples to a depth of 63.5 mm, which positions the end at the exact centre of the sample. The schematic of the samples and photo of prepared samples are shown in Figure 2.

Table 1 Rock mechanical properties

	Average UCS (MPa)	Average UTS (MPa)	Average Young's modulus (GPa)	Poisson's ratio	Average K_{Ic} (MPa$\sqrt{m}$)
Adelaide black granite	184.9	11.8	54.9	0.16	1.44

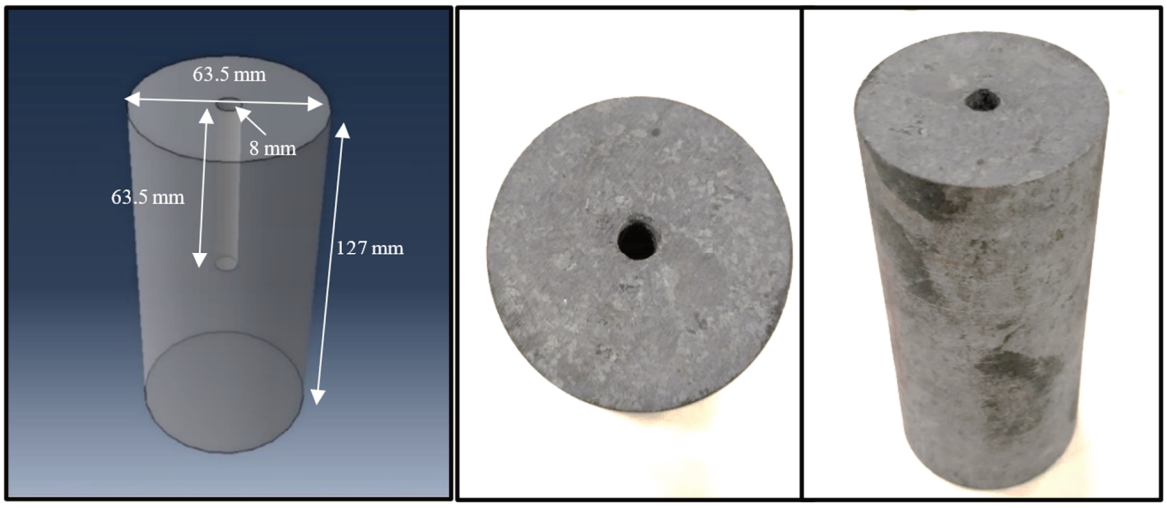

Figure 2 Schematic of the cylindrical sample with prepared samples

3.2 Experimental setup

Figure 3 illustrates the schematic of the experimental setup. The system comprises an axial loading system (Instron 1342), a confining cell (Hoek cell), rockburst test platens for holding the sample, AE sensors, Teledyne D series syringe pump for the internal pressure, syringe pump controller, AE system and the data acquisition system. The rock samples were loaded on a specially designed rockburst testing platens. The bottom platen consists of a sample holder and a 4 mm diameter hole for injecting water inside the sample. Each platen has a capacity to house four AE sensors. The axial loads are provided by the axial loading system (Instron 1342, 300 kN), which is imposed directly on the sample through the upper platens. The Hoek cell provides the confining pressure. The Teledyne D series syringe pump provides the required fluid pressure at the prescribed

injection rates, while recording the real-time pressure data, injection rate and volume from start to the end of the tests. This loading condition whereby axial stress is applied from the top, and a confining pressure is applied through the Hoek cell and the internal pressure, forms a true triaxial stress state. The data acquisition setup and the control loops are also illustrated. The control loops are shown by the solid black lines while the data acquisition loops are shown by the dotted orange lines. The AE signals are recorded by the small PICO sensors attached to the rockburst platens. The signals are amplified using an amplifier which is set to 60 dB. To cater for the mechanical noise, the lower threshold value is set to 45 dB (Karakus 2014).

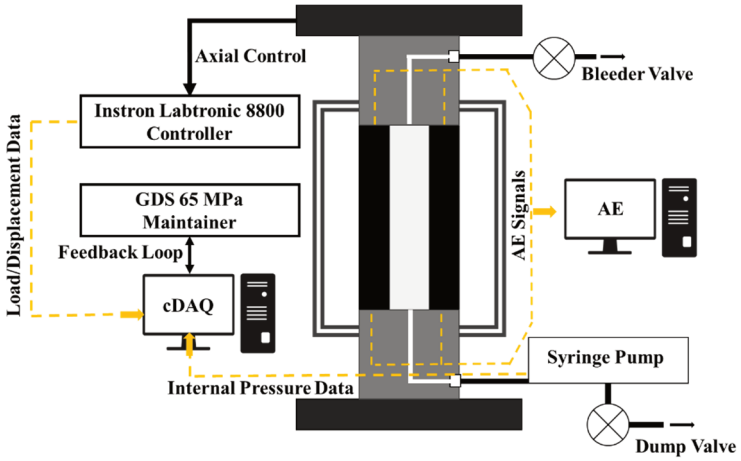

Figure 3 Schematic of the experimental setup (Bruning et al. 2018)

4 Results and discussions

4.1 Fracturing process and AE characterisation

Figure 4 illustrates the change in the internal pressure, axial, and confining pressure with time for specimen HF 5. The experiment was performed under an axial and confining stress of 20 MPa with a constant flow rate of 5 ml/min. The injection was started when the desired axial and confining pressures were achieved. It was observed that the internal pressures initially increase up to 5 MPa and then drops before it rises again. This magnitude of the pressure forces the water to infiltrate the pores and micro-cracks called the leak-off. Once the water completely infiltrates the pores and the rock is fully saturated, the internal pressure starts to increase exponentially until the specimen fails. The peak pressure at which the failure occurred is the breakdown pressure. After the breakdown is achieved a sudden drop in the internal pressure is observed due to the release of the internal pressure.

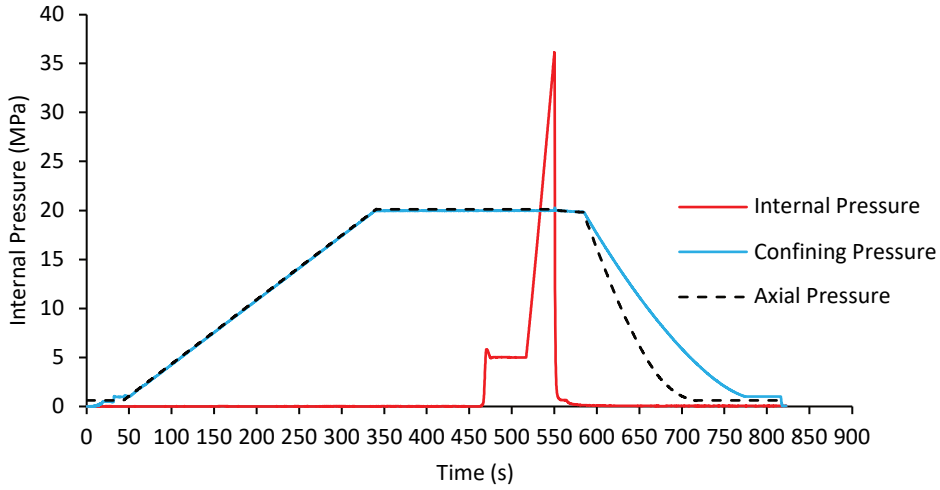

Figure 4 Variation in the breakdown, axial and confining pressure through time in sample HF5

The AE parameters during the fracturing process are shown in Figure 5. A very limited AE activity with negligible AE energy is observed up till 400 seconds whereby a surge in the AE activity is observed. As discussed above, the increase in the internal pressure results in the openings of micro-cracks within the rock structure as a result the water infiltrates inside the pores resulting in opening of pre-existing cracks and pores, which results into a surge in AE activity. After the leak-off is achieved a drop in the AE activity is observed corresponding to the pressure drop in Figure 4. An increased AE activity is observed as the pressure builds up again until the breakdown is achieved. The maximum number of hits was observed at 530 seconds which relates to the breakdown pressure and yields the maximum energy, amplitude, and frequency. It can be seen that internal pressure dropped abruptly at this stage, however, AE activity continued to be recorded up till 600 seconds which is a possible indication of the crack propagation through the specimen during the process.

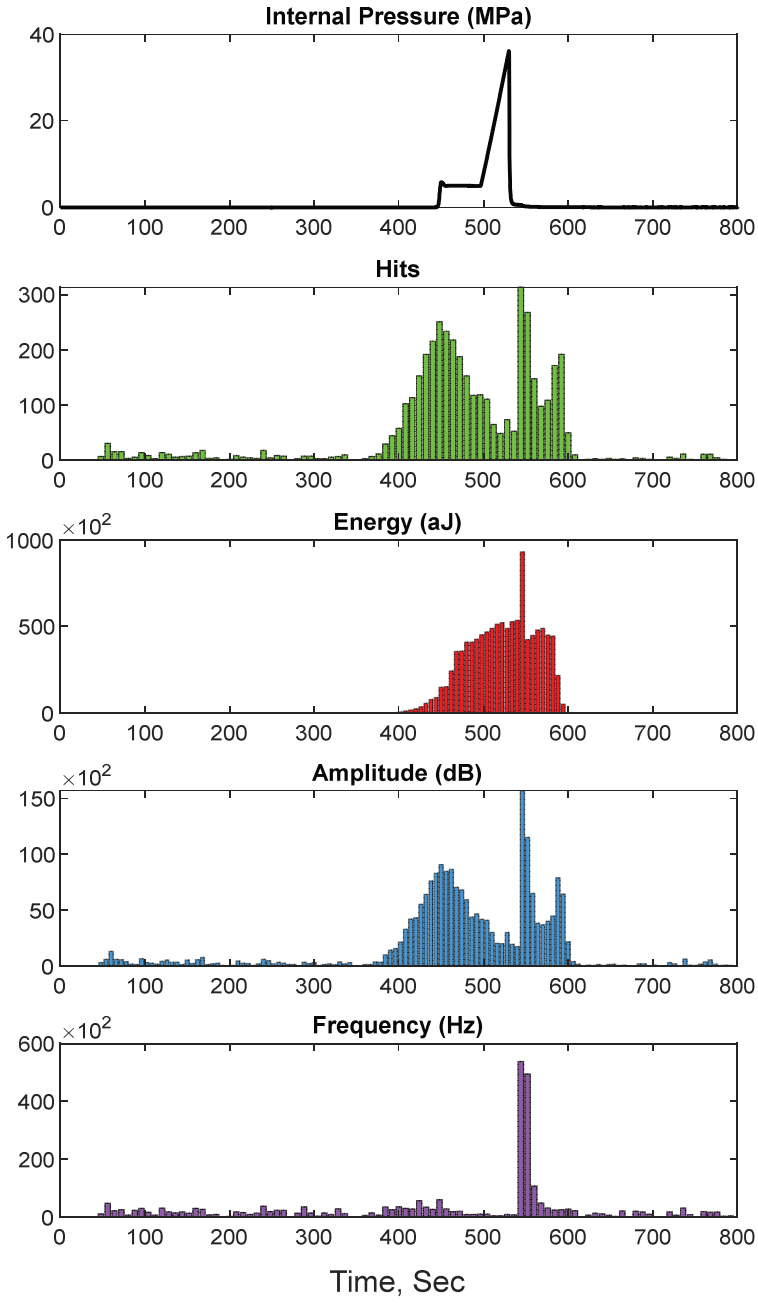

Figure 5 Change in internal pressure versus time and the corresponding AE parameters

The leak-off and breakdown can also be observed by plotting the cumulative AE hits against the time shown in Figure 6. An inflection and abrupt change in gradient are observed at the instances where leak-off and breakdown take place. On the pressure time chart, the first point of inflection corresponds to approximately

5 MPa, while the second point of inflection relates to approximately 36 MPa internal pressure which are the leak-off and breakdown pressures respectively.

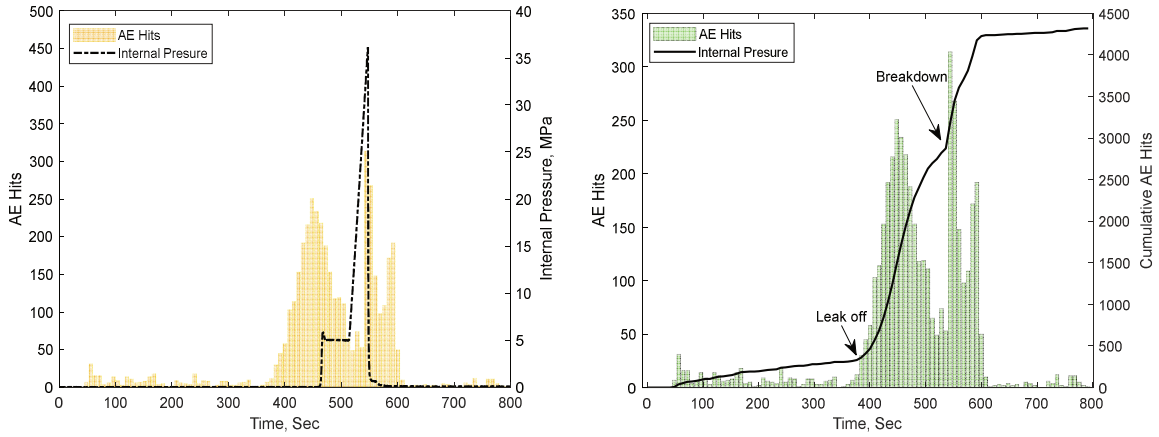

Figure 6 Plot of cumulative AE hits versus time showing point of inflection

4.2 Hydraulic fracturing results

A total of 12 hydraulic fracture tests were conducted under four different hydrostatic stress conditions. Experiments RF1 to RF3 were conducted under hydrostatic pressure of 10 MPa, RF4 to RF6 were conducted at 20 MPa hydrostatic pressure, RF7 to RF9 at 30 MPa hydrostatic pressure, and experiments RF10 to RF12 were conducted at 40 MPa hydrostatic pressure. All the tests were conducted at normal room temperature and the flow rate was kept constant at 5 ml/min which was selected based on the previous experience with the apparatus. It was observed that under hydrostatic stress conditions fractures propagate in a random direction from the weakest point around the borehole. A fractured sample from the experiments is shown in Figure 7 and results are tabulated in Table 2.

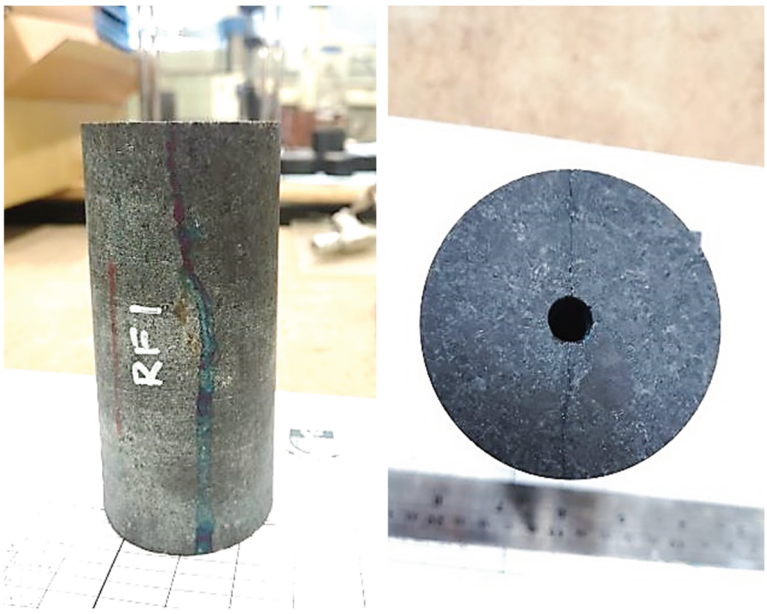

Figure 7 Fractured sample after hydraulic fracturing experiment

Table 2 Hydraulic fracturing test results

Test sample	σ_t (MPa)	K_{Ic} (MPa$\sqrt{m}$)	Flow (ml/min)	σ_1 (MPa)	σ_3 (MPa)	P_b (MPa)
RF 1	11.8	1.44	5	10	10	25.9
RF 2	11.8	1.44	5	10	10	25.8
RF 3	11.8	1.44	5	10	10	25.4
RF 5	11.8	1.44	5	20	20	36.1
RF 6	11.8	1.44	5	20	20	34.7
RF 7	11.8	1.44	5	30	30	44.9
RF 8	11.8	1.44	5	30	30	44.5
RF 9	11.8	1.44	5	30	30	42.5
RF 10	11.8	1.44	5	40	40	54.7
RF 11	11.8	1.44	5	40	40	54.7
RF 12	11.8	1.44	5	40	40	54.3

In Figure 8, the change of internal pressure against time for all of the 12 tests under different hydrostatic pressures is illustrated. It can be observed that the change in internal pressure is similar in under all the hydrostatic stress conditions. An initial increase of approximately 5 MPa is observed in the internal pressure which results in leak-off. Once the samples are fully saturated, the internal pressure increases until the tensile fracturing takes place. The leak-off happens at a constant internal pressure of 5 MPa, however, the breakdown pressures increase linearly with the degree of confinement.

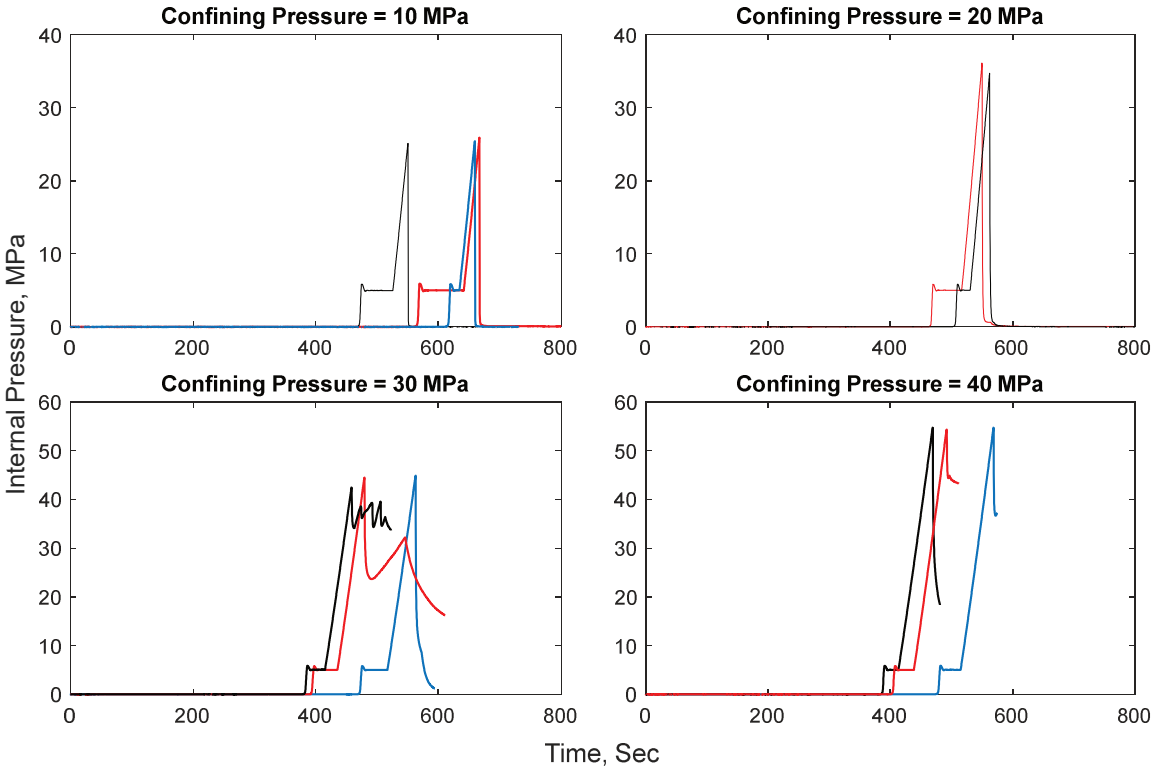

Figure 8 Plot of breakdown pressure against time under different hydrostatic pressures (axial pressure kept same as confining pressure)

The theoretical values of the breakdown pressure were predicted using the conventional theory, Haimson's approach and Adam's method which were then compared to the experimental results at each hydrostatic pressure as shown in Table 3. It was observed that with the increase in the hydrostatic pressure, there is an increase in the breakdown pressure with increments approximately equal to the stress increments.

Table 3 Theoretical and experimental breakdown pressure at different hydrostatic pressures

Method used	Hydrostatic stresses			
	10 MPa	20 MPa	30 MPa	40 MPa
P_b, conventional theory	31.8	51.8	71.8	91.8
P_b, Haimson approach	15.9	25.9	35.9	45.9
P_b, Adam's approach	25.3	35.3	45.3	55.3
P_b, experimental	25.7	35.4	43.9	54.6

Figure 9 illustrates the correlation between the breakdown pressure and the hydrostatic stresses using different approaches. The results are similar to the study conducted by Mehrgini et al. (2016) and Zhang et al. (2019) on the effect of confining pressure on the breakdown pressure of different rock types with different tensile strength and porosity. In both of these studies, a positive linear relationship was observed between the breakdown pressure and the confining pressure. The axial pressure apparently has no influence on the breakdown pressure.

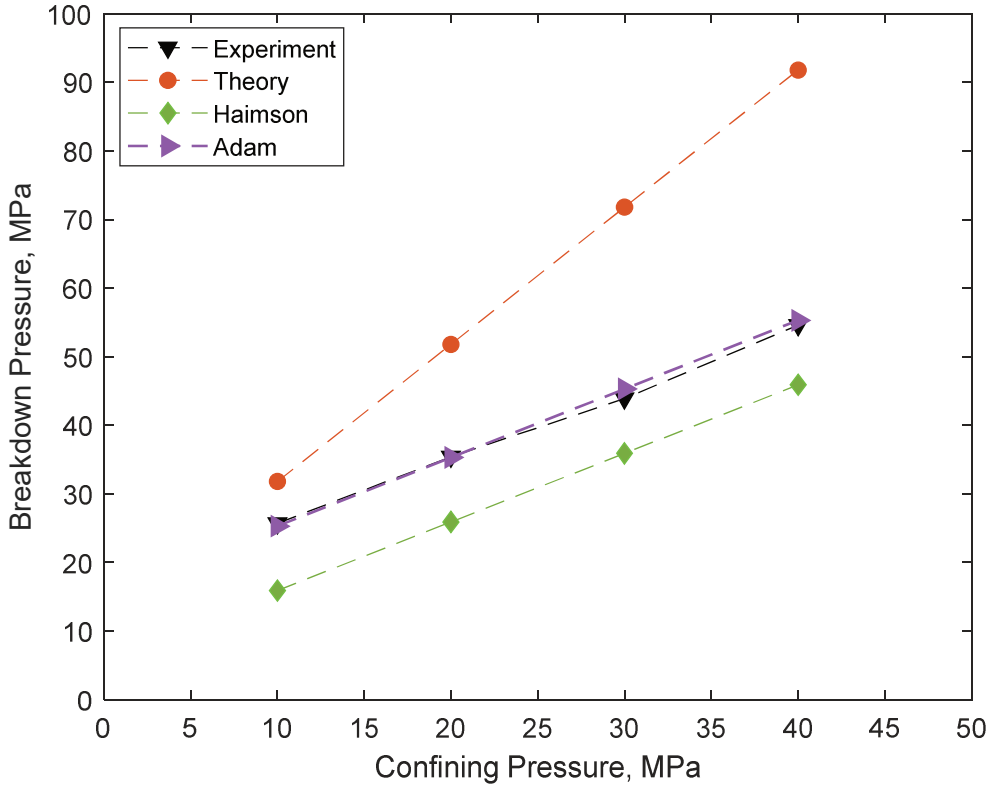

Figure 9 Comparison of theoretical and experimental breakdown pressure

According to Equation 3, this relationship between the breakdown pressure and confining stresses should be linear with a negative gradient, if σh is assumed to be zero. The relationship yields a positive linear relation with a gradient of 2 when σh is assumed to be equal to σH (hydrostatic stress). In contrast to the theory, the experimental results showed a linearly positive relation with an approximate gradient of 1 (Figure 9). Haimson's method yields a gradient of 1 but the values of breakdown pressure are

slightly lower than observed. Adam's approach based on the theory of critical distance was found accurate and consistently close to the experimental results.

As discussed in Section 2, the theoretical value of the rock tensile strength back calculated from Equation 3 (conventional theory) yields a higher value of tensile strength. This could be true as Molenda et al. (2013) showed that the tensile strength of the rock found by the Brazilian disc test is considerably lower than the hydraulic fracturing test possibly because of the compressive failure at the contact points of the specimen before the tensile failure occurs. Meanwhile, the possible higher values of the tensile strength from the hydraulic fracture test can be linked to the effect of porewater pressure which can influence the rock fracturing during the test. This is also supported by a similar study by Stoeckhert (2014) and Mehrgini (2016) on the rock tensile strength determined by the Brazilian disc test and the unconfined hydraulic fracture test, where it was found that the breakdown pressure was slightly higher than the Brazilian disc test results for most of the rocks as shown in Figure 10.

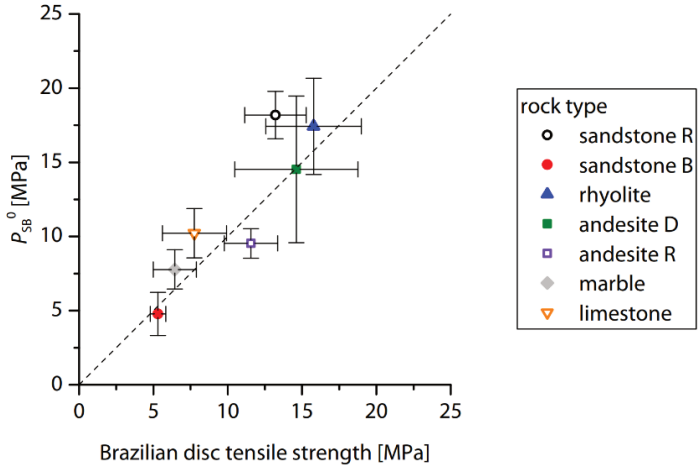

Figure 10 Hydraulic and Brazilian tensile strength of rock (Stoeckhert 2014)

5 Conclusion

Hydraulic fracturing is widely used around the world for cave propagation in block cave mining and rockburst risk mitigation in high stress working environments. If properly planned and executed, the process can improve caveability, rock fragmentation and mitigate seismic risks. This research compares various breakdown models for intact rock to ascertain a best-fit for optimal design at field scale. The effect of in situ stress conditions and rock tensile strength were studied under fixed injection rate. It was found that the breakdown pressure increases linearly with the increase in the degree of confinement or the hydrostatic stress state. Adam's model based on the theory of critical distances could precisely predict the breakdown pressure for the intact rock under hydrostatic stress conditions. The conventional theory predicted values much higher than the experiment results, while the Haimson's method yielded lower values. Also, it was observed that the conventional theory yields higher values of rock tensile strength when back calculated from the equation. This could be true under unconfined conditions as the possible lower values of tensile strength from the Brazilian disc tests are because of the compressive failure at the contact points of the specimen before the tensile failure occurs, which could be further investigated. Further, under the hydrostatic stress conditions, the fractures initiated and propagated in a random direction from the weakest point around the borehole. This could be verified by extended finite element modelling (XFEM) which is a future goal of this study.

Acknowledgement

The authors are grateful to the OZ Minerals for providing funds to support this research. The authors also like to thank and acknowledge Adam Ryntjes and Jon Ayoub for their help in conducting the experiments.

References

Adam, KS, Nouné SM, Chaoshui Xu 2017, 'Fracture mechanics approximation to predict the breakdown pressure using the theory of critical distances', *International Journal of Rock Mechanics and Mining Sciences*, vol. 95, pp.48–61.

Ali, Z, Karakus, M, Nguyen, GD & Amrouch, K 2022, 'Application of full-field strain measurement to study Kaiser effect in granite under indirect tensile loading', *Proceedings* of the *56th US Rock mechanics/Geomechanics Symposium*, American Rock Mechanics Association, Alexandria.

Brady, BHG & Brown, ET 1999, *Rock Mechanics: For Underground Mining*, 2nd edn, Springer, Dordrecht.

Bruning, T, Karakus, M, Nguyen, GD, Akdag, S & Goodchild, D 2018, 'Influence of deviatoric stress on rock burst occurrence: An experimental study', *International Journal of Mining Science and Technology,* vol. 28, no. 5, pp. 763–766.

Brzovic, A, Rogers S, Webb, G, Hurtado, JP, Marin, N, Schachter, P & Baraona, K 2015, 'Discrete fracture network modelling to quantify rock mass pre-conditioning at the El Teniente Mine, Chile', *Mining Technology*, vol. 124, no. 3, pp. 163–177.

Bunger, A, Zhang, X & Jeffrey, RG 2011, 'Parameters effecting the interaction among closely spaced hydraulic fractures', paper presented at the SPE Hydraulic Fracturing Technology Conference, Woodland, Texas, Society of Petroleum Engineers.

Chacon, E, Jeffrey, R, van AA 2004, 'Hydraulic fracturing used to precondition ore and reduce fragment size for block caving', *Proceedings of MassMin 2004,* Instituto de Ingenieros de Chile, Santiago, pp. 529–534.

Clark, J B 1949, 'A hydraulic process for increasing the productivity of wells', *Journal of Petroleum Technology,* vol. 1, no. 1, pp. 2180–2207.

Catalan, A, Onederra, I & Chitombo, G 2017a, 'Evaluation of intensive preconditioning in block and panel caving – Part I, quantifying the effect on intact rock', *Mining Technology*, pp. 1–12.

Haimson, BC & Fairhurst, C 1967, 'Initiation and extension of hydraulic fractures in rocks', *Society of Petroleum Engineers Journal*, SPE 1710-PA.

He, Q, Suorineni, FT & Oh, J 2016a, 'Review of hydraulic fracturing for preconditioning in cave mining', *Rock Mechanics and Rock Engineering*, vol. 49, no. 12, pp. 4893–4910.

Jeffrey, R, Zhang, X & Chen, Z 2017, 'Hydraulic fracture growth in naturally fractured rock Porous Rock', *Fracture Mechanics*, pp. 93–116.

Juncal, A, Ivars, D, Brzovic, A & Vallejos, J 2014, 'Simulating the effect of preconditioning in primary fragmentation: structures in and on rock masses, *Rock Mechanics and Rock Engineering,* pp. 661–665.

Karakus, M 2014, 'Quantifying the discrepancy in preloads estimated by acoustic emission and deformation rate analysis', paper presented at the *International Society of Rock Mechanics, European Rock Mechanics Symposium,* Vigo, Spain.

Katsaga, T, Riahi A, DeGagne, DO, Valley, B & Damjanac, B 2015, 'Hydraulic fracturing operations in mining: conceptual approach and DFN modelling example', *Mining Technology*, vol. 124, no. 4, pp. 255–266.

Mehrgini, B, Memarian, H, Memarian, H, Goodarzi B, Eshraghi, H, Ghavidel, A, Hassanzade, M & Niknejad, M 2016, 'Comparing laboratory hydraulic fracturing and Brazilian test tensile strengths', paper presented at the *50th US Rock Mechanics/Geomechanics Symposium,* Houston, Texas, USA.

Mills, K 2004, 'Remote high resolution stress change monitoring for hydraulic fractures', in A Karzulovic & MA Alfaro (eds), *Proceedings of MassMin 2004,* Instituto de Ingenieros de Chile, Santiago, pp. 529–534.

Molenda, M, Brenne, S & Alber, M 2013, *Effective and Sustainable Hydraulic Fracturing*, Intech Open Limited.

Stoeckhert, F, Brenne, S, Molenda, M & Alber, M 2014, 'Hydraulic fracturing – laboratory experiments, acoustic emissions, and fracture mechanics', *Geomechanik Kolloquium*, TU Bergakademie Freiberg, pp. 79–105.

Zhai, C, Li, M, Sun, C, Zhang, J, Yang, W & Li, Q 2012, 'Guiding-controlling technology of coal seam hydraulic fracturing fractures extension', *International Journal of Mining Science and Technology*, vol. 22, no. 6, pp. 831–836.

Zhang, Y, Hu, Z, Lei, H, Bai, L, Lei, Z & Zhang, Q 2019, 'An experimental investigation into the characteristics of hydraulic fracturing and fracture permeability after hydraulic fracturing in granite', *Renewable Energy*, vol. 140, pp. 615–624.